

A study of the response of $\text{Y}_3\text{Al}_5\text{O}_{12}:\text{Ce}$ phosphor powder screens in the vacuum ultraviolet and soft X-ray regions using synchrotron radiation

A. Baciero,^{a*} K. J. McCarthy,^a M. A. Acedo,^a L. Rodriguez-Barquero,^b J. Avila,^{c,d} Y. Huttel,^{c,d} V. Perez Dieste,^c M. C. Asensio^{c,d} and B. Zurro^a

^aLaboratorio Nacional de Fusión, Asociación Euratom-CIEMAT, Avenida Complutense 22, 28040 Madrid, Spain, ^bUnidad de Radiaciones Ionizantes, CIEMAT, Avenida Complutense 22, 28040 Madrid, Spain, ^cLURE, Bâtiment 209D, Centre Universitaire Paris-Sud, 91405 Orsay, France, and ^dInstituto de Ciencia de Materiales, CSIC, 28049 Madrid, Spain.
E-mail: alfonso.baciero@ciemat.es

(Received 29 November 1999; accepted 2 May 2000)

Phosphor screens find application in many fields because of their ability to convert incident radiation to wavelengths that are readily measured by modern detectors. While the response of such screens in the X-ray region has been widely studied, much work still remains to be done regarding their response in the vacuum ultraviolet and soft X-ray regions, where the response is predicted to be non-linear owing to the presence of elemental absorption edges. Here, an experiment using synchrotron radiation to determine the response of thin $\text{Y}_3\text{Al}_5\text{O}_{12}:\text{Ce}$ ($1\text{--}21\text{ mg cm}^{-2}$) and $\text{Y}_2\text{O}_3:\text{Eu}$ (2.64 mg cm^{-2}) powder phosphor screens in the spectral range $20\text{--}900\text{ \AA}$ ($13.8\text{--}620\text{ eV}$) is reported. Also, a custom-built camera is described which permits simultaneous collection of the forward- and backward-emitted light and that enables measurements to be made at various positions across the screens and at several screen/incident beam angles. Finally, features in the response spectra are identified, and efficiencies across the spectral range indicated for different screen thicknesses and operating modes are plotted, before a curve of the intrinsic radiant efficiency of $\text{Y}_3\text{Al}_5\text{O}_{12}:\text{Ce}$ is produced. The results are discussed in the context of other measurements.

Keywords: phosphor powder; photoluminescence; VUV; efficiency measurements; plasmas.

1. Introduction

For many years phosphor powders have been used in fluorescent lamps, televisions and medical diagnostics, while more recently they have been applied to high-energy and nuclear physics to convert incident radiation to wavelengths that can be readily measured by modern detectors (Blasse & Grabmaier, 1994; Murakami, 1998). They have also found application as broadband radiation detectors in plasma fusion devices because of their immunity to electromagnetic interference and ground loops, radiation hardness [for example, $\text{Al}_2\text{O}_3:\text{Cr}$ screens are quoted as having a radiation-resistant limit of $10^{18}\text{--}10^{19}$ protons cm^{-2} (Johnson, 1990)] and compactness since only a thin screen needs to be close to the plasma (Zurro, Burgos, Ibarra & McCarthy, 1997). Furthermore, several phosphors can be heated to 423 K (during vacuum-chamber bakeout) with little or no observed changes in their decay times and luminescence intensity. One such phosphor is $\text{Y}_3\text{Al}_5\text{O}_{12}:\text{Ce}$, commonly known as P46. Owing to its very fast decay time, $\sim 150\text{ ns}$, it has been selected for the Spanish TJ-II stellarator (Alejaldre *et al.*, 1999), where plasma lifetimes are short, typically $\leq 500\text{ ms}$. Indeed, several thin screen-based

detector systems have been designed to monitor vacuum ultraviolet (VUV) and soft X-ray radiation emitted by highly ionized impurity and metal ions in TJ-II plasmas (Zurro, Burgos, McCarthy & Rodriguez Barquero, 1997).

In a previous paper we reported on measurements made on several screens of $\text{Y}_3\text{Al}_5\text{O}_{12}:\text{Ce}$ ($1\text{--}21\text{ mg cm}^{-2}$) under excitation by X-ray radiation between 20 and 50 keV, and discrete VUV lines between 10 and 27 eV ($461\text{--}1211\text{ \AA}$) (Baciero *et al.*, 1999). Luminescence efficiencies for both forward and backward modes (also called transmission and reflection modes) were determined by collecting the luminescent light emitted from the front and back of the screens and the results were used to obtain fitting parameters for a granular unidimensional radiation-transfer model. The model developed therein took into account the effects of scattering and absorption of the emitted luminescent light and considered the effects of grain size and shape. A plot of optimized screen thickness, for maximum signal-to-noise ratio, *versus* incident radiation energy was then created for the forward mode. With it, screen thicknesses can be tailored to the radiation energy range of interest. However, as with most broadband detectors, it is necessary to characterize their response across their full operational wave-

length range. This is the case here, where the response in the VUV and soft X-ray range is expected to be non-linear due to surface effects, absorption edges *etc.* To our knowledge, the response of $\text{Y}_3\text{Al}_5\text{O}_{12}:\text{Ce}$ has not been studied in this range. Indeed, only a few studies have been made to characterize phosphors in this range. Of those made, we cite the work of Benitez *et al.* (1991), who studied the response of several luminescent materials between 27.5 and 729 Å (17 and 450 eV) using synchrotron radiation, that of Chappell & Murray (1984), who made spot transmission measurements on several high-efficiency rare-earth phosphors between 0.7 and 6 keV, that of Berkowitz & Olsen (1991), who measured the absolute quantum efficiencies of some well known phosphors between 500 and 2480 Å (5–25 eV), and that of Popma *et al.* (1981), who collected emission spectra of several phosphors, including $\text{Y}_3\text{Al}_5\text{O}_{12}:\text{Ce}$, between 200 and 3000 Å (4–60 eV).

In this work we present measurements made using synchrotron radiation on three $\text{Y}_3\text{Al}_5\text{O}_{12}:\text{Ce}$ phosphor powder screens ($1\text{--}21\text{ mg cm}^{-2}$) over the range from 20 to 900 Å (13.8–620 eV), and we describe a custom-built camera that allows backward- and forward-emitted light to be collected simultaneously. From the data, we determine the quantum efficiencies of the screens, and we use the model developed by Baciero *et al.* (1999) to produce fits and to produce a curve of the intrinsic luminescence efficiency of this phosphor. In addition, we attempt to identify the features present in the phosphor excitation spectrum. Finally, we report on measurements made on a thin screen

of the phosphor $\text{Y}_2\text{O}_3:\text{Eu}$, known as P22R, over the same energy range, and we compare these measurements with those cited by Benitez *et al.* (1991), Chappell & Murray (1984) and Berkowitz & Olsen (1991).

2. Experiment

The photoluminescence measurements were made on the Spanish–French beamline SU8 installed at the SUPER-ACO storage ring in LURE-Orsay, France. The beamline is basically composed of an undulator wiggler to ensure an elevated photon flux in the energy range from 13 to 900 eV. A monochromatic beam is extracted from the synchrotron beam by passing it through six varied-line-spacing (VLS) plane-grating monochromators (PGM). Toroidal mirrors, in astigmatic mode, are used as pre- and post-focusing optics to form independent source images in the vertical and horizontal planes at the experimental point.

The sample under investigation was placed in a custom in-house vacuum chamber consisting of a five-way vacuum cross (model CX5-63 by Caburn-MDC, England) mounted on a specially adapted XY translation support table. One arm of the vacuum cross was coupled *via* a flexible vacuum bellows to the end of the beamline (see Fig. 1). The sample, which was held in a 50 mm-diameter sample holder, was fixed to the end of a combined rotary and linear motion feedthrough (model VF-180-3 by Huntington) that was mounted on a second arm of the five-way cross. This system permitted measurements to be made at a number of positions across the sample (so that any pinholes or non-uniformities in the screen could be cancelled) as well as at different screen/incident beam angles. Two photomultiplier tubes (PMTs) (model H5783-04 by Hamamatsu) located on the outside of in-house-designed zero-length viewports, that were mounted at the ends of the third and fourth arms, measured the light emitted from the sample in the forward and backward directions. The signal currents from the PMTs were measured using picoammeters (model 485 by Keithley). Note that two apertures, located between the sample and detectors, minimized reflections off the chamber walls. Finally, a turbomolecular pump was connected to the fifth arm. No filters were present between the grating and sample chamber to protect the vacuum and cleanliness integrity of the beamline, so it was necessary to bake the sample chamber at 423 K for several hours prior to opening it to the beamline.

For this work, $\text{Y}_3\text{Al}_5\text{O}_{12}:\text{Ce}$ (P46) phosphor samples were prepared on 48 mm-diameter ultrahigh-purity quartz plates (spectrosil by Dynasil) using an in-house sedimentation technique. This consisted of dispersing some powder in an aqueous solution which was shaken and heated before being deposited over the plates. After sedimentation the excess was drained off and the samples were heated to 413 K for a short period (Zurro, Burgos, McCarthy & Rodriguez Barquero, 1997). In total, three 30 mm-diameter screens of thicknesses 1.33, 3.37 and 20.56 mg cm^{-2} were studied. The uniformity of the screens

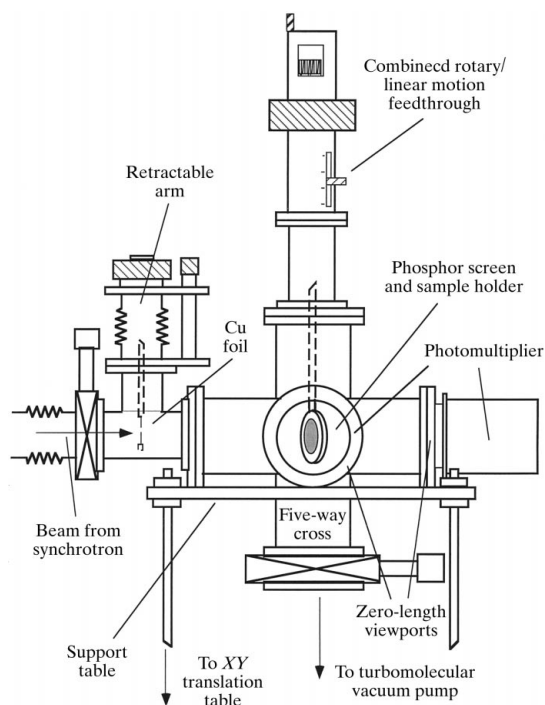


Figure 1
Schematic diagram of the custom vacuum chamber and accessories attached to the end of beamline SU8.

Table 1

Grating ranges and step sizes for measurements made on beamline SU8.

Grating	Energy range (eV)	Step size (eV)
R1	13.8–35.5	0.2
R2	33.5–82.8	0.5
R3	62.1–155.3	0.5
R4	138–310.6	1.15
R5	276.1–621.1	2

was checked by optical absorption in the visible and uniformities of about 1% were typically achieved. The luminescence emission of the $\text{Y}_3\text{Al}_5\text{O}_{12}:\text{Ce}$ phosphor, which arises from transitions from the lowest $5d$ state ($5d_1$) to the $4f$ ground state of Ce^{3+} , peaks near 5500 \AA at room temperature (Blasse & Grabmaier, 1994). In addition, this phosphor has a 10% luminescence decay time of 150 ns and an energy efficiency of 3.3% (equivalent to a light yield of 1.4×10^4 photons MeV^{-1}). The phosphor powder, as supplied by Phosphor Technology Ltd (type OMK58), had a stated Ce concentration of $\sim 0.4\%$ mole, an average grain size of $6.6 \mu\text{m}$ [the model of Baciero *et al.* (1999) uses a value of $1.7 \mu\text{m}$], a quartile deviation of 0.28 and a density of 4.15 g cm^{-3} (Phosphor Technology Ltd, Nazeing, UK; Technical Data Sheet OMK58). In addition, one $\text{Y}_2\text{O}_3:\text{Eu}$ (P22R) screen with 2.64 mg cm^{-2} was prepared in the manner outlined previously. The luminescence emission of this phosphor peaks near 6110 \AA at room temperature and arises principally from the $^5D_0-^7F_2$ transition of Eu^{3+} . This phosphor has a 10% luminescence decay time of $\sim 1 \text{ ms}$, and an energy efficiency of 8.7% (equivalent to a light yield of 4.3×10^4 photons MeV^{-1}). The powder, which was a commercial sample, was supplied by Osram Sylvania Inc. and had a Eu concentration of 4% mole and a density of 4.8 g cm^{-3} (Osram Sylvania Inc., 1993).

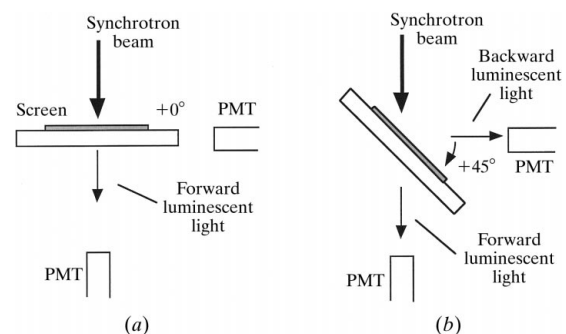
Energy scans were made with the phosphors at room temperature using the monochromatic beam over the energy ranges shown in Table 1. The incident beam flux was determined by measuring the replacement current, I_0 , in a 1 mm-thick Cu foil mounted on a retractable arm positioned between the sample chamber and grating monochromator (see Fig. 1). An autoranging picoammeter (model 485 by Keithley) was used for this. Although no light filters were present in the beamline, background light levels were minimal. Finally, the synchrotron beam size on the screen was determined to be $\sim 0.1 \text{ cm}^2$ by translating the sample chamber while viewing the beam through the zero-length windows. The results of the energy scans and the corrections made to the data are now presented.

3. Results and analysis

Measurements of the phosphor screen response were made for three different incident beam/screen angles (see Fig. 2). In the first instance the phosphor screen was rotated so that its surface normal was parallel to the incident-light beam

direction. In this set-up only forward luminescent light emitted by the screen was recorded. In addition, measurements were made at several positions across each screen in order to determine the uniformity of the screen response. In all cases the monochromatic beam intercepted the phosphor screen close to its centre and the variation in response was found to be within the experimental error. In the second instance the phosphor screen was rotated so that its surface normal was at $+45^\circ$ to the incident beam and signals from both PMTs were recorded. For this case the increased screen thickness must be considered when analysing or modelling the phosphor response. Finally, measurements were also made for the phosphor at -45° to the incident beam, in order to compare the relative response of the two PMT detectors. The difference was found to be less than 3%.

When post-processing the data, several corrections were made to the measured signals. Firstly, to compensate for beam intensity decay during the experiment, correction factors, determined from the stored ring current, were applied. Secondly, the photon flux incident on the detectors was estimated using PMT sensitivity curves (Hamamatsu Photonics KK, 1996). Note that the background PMT signal was $<0.1\%$ of the luminescence light signals. Corrections were also applied for transmission and reflective signal losses in the screen support plate and viewports (both spectrosil) (Baciero *et al.*, 1999). From the known screen/PMT geometry and the Lambertian fall-off in observed light intensity as a function of view angle, the light emitted by the screen over 2π steradians in the backward and forward modes was determined for each set-up. Thirdly, the synchrotron light spectrum was determined from the replacement current, I_0 , in the Cu foil. Quantum efficiency curves, *i.e.* the number of electrons emitted from the foil surface per incident photon, by Cairns & Samson (1966) and Day *et al.* (1981), were used for this purpose. The copper sample consisted of a pure polycrystalline foil chemically cleaned with ethanol and acetone prior to introduction to the vacuum system. In the range 14–50 eV, reflectance of incident light off the phosphor screen was

**Figure 2**

Schematic diagrams showing incident, forward and backward radiation directions for the synchrotron beam/screen orientations; (a) 0° , (b) $+45^\circ$.

also considered (Benitez *et al.*, 1991). Finally, curves of phosphor quantum efficiencies (number of visible photons emitted per incident photon) were created by splicing together scans from overlapping energy ranges.

In Figs. 3–6 we present measured quantum efficiencies for the Y₃Al₅O₁₂:Ce and Y₂O₃:Eu screens. The uncertainties in the measurements used to create the error bars are shown in Table 2. In Figs. 3 and 5, two sets of curves are presented. They represent the response for the backward and forward modes for the +45° case. Note that the total number of photons emitted from the screen per incident photon is simply a sum of these two curves. In Figs. 4 and 6 the curves represent the response in the forward mode for 0°. Several features are apparent in these curves, *e.g.* the peaked feature centred about ~28.5 eV in Y₃Al₅O₁₂:Ce and about ~29.3 eV in Y₂O₃:Eu. A similar feature was seen by Popma *et al.* (1981), although at a lower energy, and was attributed to an increase in excitation of core levels in the

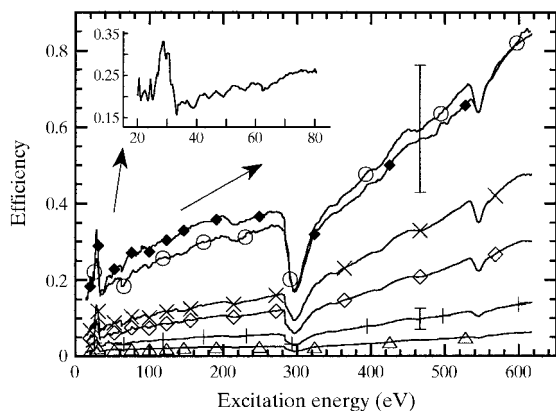


Figure 3
Y₃Al₅O₁₂:Ce efficiencies (photons emitted per incident photon) as a function of excitation energy in forward and backward modes for 1.33 (◇ and ×), 3.37 (+ and ○) and 20.56 mg cm⁻² (△ and ◆) screens at 45°. Error bars are shown for two cases. Backward mode efficiencies between 20 and 80 eV for the 20.56 mg cm⁻² screen are expanded.

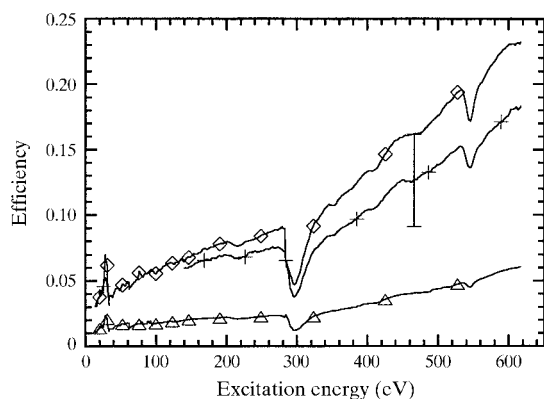


Figure 4
Y₃Al₅O₁₂:Ce efficiencies in forward mode for 1.33 (◇), 3.37 (+) and 20.56 mg cm⁻² (△) screens at 0°.

Table 2
Principal sources of error in measurements.

Equipment/measurement	Uncertainty (%)
PMT sensitivity	20
PMT current	<0.2
Cu foil quantum efficiency	20
Cu foil current	<1
Quartz plate (reflectance, transmission)	<1
Screen angle	2.5
Screen thickness	<1

activator. However, in both our phosphors the peak is displaced here by several eV to a region between ~25 and 35 eV where increased yttrium absorption occurs, *i.e.* just above the yttrium *N*-absorption edges at 23.1 and 24.4 eV (Tomiki *et al.*, 1989). In this region the efficiency of energy transfer from the host lattice to the activator is maximum (Ilmas & Savikhina, 1970) and, hence, we believe that the increased host lattice absorption is the cause of the features observed. Also, for several tens of eV above the peak,

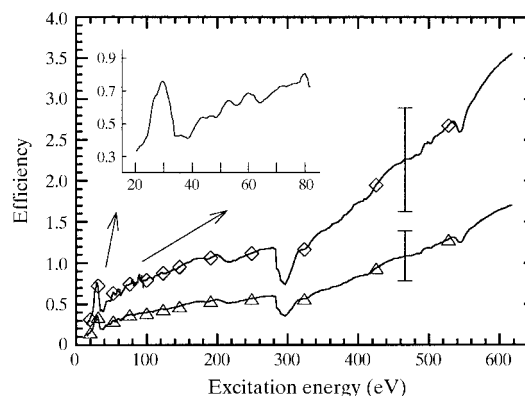


Figure 5
Y₂O₃:Eu efficiencies in forward and backward modes for the 2.64 mg cm⁻² (△ and ◇) screen at 45°. The backward mode efficiencies are expanded between 20 and 80 eV.

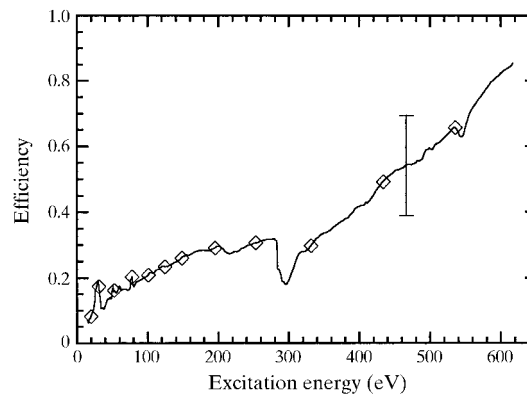


Figure 6
Y₂O₃:Eu efficiencies in forward mode for the 2.64 mg cm⁻² (◇) screen at 0°.

small-scale structures are seen every 5–7 eV. These may be associated with interband Auger multiphoton emission processes, *i.e.* a stepped increase with energy in the number of visible photons produced by every VUV photon absorbed that leads to luminescence (Ilmas & Savikhina, 1970). These structures have a repetition rate close to the host bandgap energy, *i.e.* $E_{gP(46)} \simeq 6.3$ eV (Hurrell *et al.*, 1968) and $E_{gP(22R)}$ is between 5.6 eV (Alig & Bloom, 1977) and 6.25 eV (Berkowitz & Olsen, 1991). The other prominent features near 282 eV and 530 eV correspond to the C and O *K*-absorption edges, respectively. There is also structure, associated with the extended X-ray absorption fine structures (EXAFS) of both carbon and oxygen, that extends to ~ 100 eV about these edges. Here, carbon is a contaminant that gives rise to reduced output efficiency just above 282 eV and whose origin is due to the processes used in the fabrication of the phosphors (Benitez *et al.*, 1991). We estimate a 0.5–1% molar concentration of carbon. Weaker features, about 200 and 425 eV, have not been identified. Another interesting feature in Fig. 3 is the increased backward mode efficiency of the 3.37 mg cm^{-2} screen between 300 and 520 eV. We attribute this to reflection of visible light off the support plate rather than to luminescence of the same. Note that spectrosil does not exhibit luminescence under UV radiation (Dynasil Corporation, Berlin, New Jersey, USA; Fused Silica Catalog 702-B) or hard X-ray radiation. In the case of the thicker screen, this reflected light is attenuated because of the longer path length. Finally, using the data for forward and backward modes, the intrinsic luminescence efficiency of $\text{Y}_3\text{Al}_5\text{O}_{12}:\text{Ce}$ was determined for each energy step using the granular unidimensional model by Baciero *et al.* (1999). This process, when repeated for each energy step between 14 and 620 eV, produced the intrinsic luminescence efficiency (η_c) curve shown in Fig. 7. This curve, which is independent of screen thickness, is the sum of two contributions (Leverenz, 1968). Firstly, photoluminescence, where an absorbed incident photon directly creates a

visible photon with efficiency (η_p). Secondly, roentgenoluminescence, where an absorbed incident photon creates a free internal electron that in turn creates many internal secondary electrons which produce visible photons with efficiency (η_{rgn}). Their sum, the intrinsic efficiency, is given by

$$\eta_c = \eta_p(E_v/E) + \eta_{rgn}, \quad (1)$$

where E_v and E are the visible and absorbed photon energies, respectively. The course of the intrinsic efficiency curve is dominated by (E_v/E) up to several hundred eV, beyond which roentgenoluminescence becomes increasingly important.

Although direct comparisons cannot be made for $\text{Y}_3\text{Al}_5\text{O}_{12}:\text{Ce}$ efficiencies, we can compare our measured $\text{Y}_2\text{O}_3:\text{Eu}$ efficiencies with those of Benitez *et al.* (1991), Chappell & Murray (1984) and Berkowitz & Olsen (1991). In the first instance we see a large discrepancy (a factor of ~ 7) between our efficiencies and those of Benitez *et al.* (1991). In this case we believe that the values reported may be too high and we estimate that their intrinsic efficiency, ~ 0.113 , is greater than the generally accepted maximum value for this phosphor, *i.e.* 0.087 (Blasse & Grabmaier, 1994). In addition, their sample had a higher Eu concentration (6% molar) while the carbon contamination concentration appears, from the edge jump in their Fig. 2, to be much lower. A higher concentration of impurities can lead to an increase in the number of defects and trapping centres and hence a loss in visible photon emission while a larger activator concentration, up to a point, increases the probability of recombination at an activator site (Berkowitz & Olsen, 1991; Popma *et al.*, 1981). In contrast, our results, when extrapolated to 6 keV, appear to be significantly higher (by a factor of ~ 4) than the P22R and P46 efficiencies determined by Chappell & Murray (1984) for transmission mode. Finally, between 14 and 25 eV our results, when extrapolated to their screen thickness of 1.5 mm, appear to be in reasonable agreement (within a factor of ~ 2) with those of Berkowitz & Olsen (1991) made in reflection mode. In conclusion, measurements on $\text{Y}_2\text{O}_3:\text{Eu}$ phosphor screens have produced a broad range of efficiencies to date, which makes it difficult to make comparisons. While this may be due in part to phosphors from different manufacturers, as well as to different screen preparation techniques, the measurements reported have been made on single screens and in each case in only one mode.

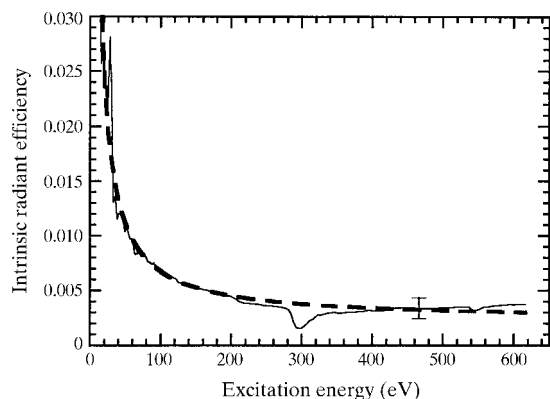


Figure 7

$\text{Y}_3\text{Al}_5\text{O}_{12}:\text{Ce}$ intrinsic radiant efficiencies between 14 and 620 eV. This curve is independent of screen thickness. Also shown is the fitted curve (broken line) used to obtain the values for η_p and η_{rgn} , *i.e.* 0.19 and 0.0023, respectively.

4. Conclusions

The intrinsic efficiencies of the phosphor $\text{Y}_3\text{Al}_5\text{O}_{12}:\text{Ce}$ have been determined in the range 20–900 Å (13.8–620 eV) using synchrotron radiation. When compared with phosphors normally used in this range, for instance $\text{Y}_2\text{O}_3:\text{Tb}$ (P45), the relative efficiency is an order of magnitude lower (Chappell & Murray, 1984). However, $\text{Y}_3\text{Al}_5\text{O}_{12}:\text{Ce}$ screens can be used in applications where a very fast response time

(<1 μs for P46 compared with ~1 ms for P45) can be traded off at the expense of conversion efficiency. Indeed, this is the case for a new system, based on a toroidal mirror and a P46 screen, that operates in backward mode and that provides limited spatial resolution, and which will be described in a later publication.

Finally, further work, involving a comparison of material from different manufactures or produced by different methods, might help to clarify the reasons for the broad range of efficiencies measured. In addition, measurements on phosphor screens should be performed in both forward and backward modes, and on a range of screen thicknesses, in order to avoid possible overestimates or underestimates.

This work was supported by the Training and Mobility of Researchers (TMR) Programme of the European Community and was partially funded by the Spanish Ministry of Science and Education under contract DGCYT No. PB 94-1229. AB is supported by a scholarship from the Institute of Energy Studies.

References

- Alejandre, C., Alonso, J., Almoquera, L., Ascasfbar, E., Baciero, A., Balbín, R., Blaumoser, M., Botija, J., Brañas, B., de la Cal, E., Cappa, A., Carrasco, R., Castejón, F., Cepero, J. R., Cremy, C., Doncel, J., Dulya, C., Estrada, T., Fernández, A., Francés, M., Fuentes, C., García, A., García-Cortes, I., Guasp, J., Herranz, J., Hidalgo, C., Jiménez, J. A., Kirpichev, I., Krivenski, V., Labrador, I., Lapayse, F., Likin, K., Liniers, M., López-Fraguas, A., López-Sánchez, A., de la Luna, E., Martín, R., Martínez, A., Medrano, M., Méndez, P., McCarthy, K., Medina, P., van Milligen, B., Ochando, M., Pacios, L., Pastor, I., Pedrosa, M. A., de la Peña, A., Portas, A., Qin, J., Rodríguez-Rodrigo, L., Salas, A., Sánchez, E., Sánchez, J., Tabarés, F., Tafalla, D., Tribaldos, V., Vega, J., Zurro, B., Akulina, D., Fedyanin, O. I., Grebenshchicov, S., Kharchev, N., Meshcheryakov, A., Barth, R., van Dijk, G., van der Meiden, H. & Petrov, S. (1999). *Plasma Phys. Control. Fusion*, **41**, A539–A548.
- Alig, R. C. & Bloom, S. (1997). *J. Electrochem. Soc.* **124**, 1136–1138.
- Baciero, A., Placentino, L., McCarthy, K. J., Barquero, L. R., Ibarra, I. & Zurro, B. (1999). *J. Appl. Phys.* **85**, 6790–6796.
- Benitez, E. L., Husk, D. E., Schnatterly, S. E. & Tarrío, C. (1991). *J. Appl. Phys.* **70**, 3256–3260.
- Berkowitz, J. K. & Olsen, J. A. (1991). *J. Lumin.* **50**, 111–121.
- Blasse, G. & Grabmaier, B. C. (1994). *Luminescent Materials*, 1st ed. Berlin: Springer.
- Cairns, R. B. & Samson, J. A. R. (1966). *J. Opt. Soc. Am.* **56**, 1568–1573.
- Chappell, J. H. & Murray, S. S. (1984). *Nucl. Instrum. Methods*, **221**, 159–167.
- Day, R. H., Lee, P., Saloman, E. B. & Nagel, D. J. (1981). *J. Appl. Phys.* **52**, 6965–6973.
- Hamamatsu Photonics KK (1996). Photosensor Module H5783 Series, Technical data sheet (TPMHB0293EA). Hamamatsu Photonics KK, Shizuoka-ken, Japan.
- Hurrell, J. P., Porto, S. P. S., Chang, I. F., Mitra, S. S. & Baumar, R. P. (1968). *Phys. Rev.* **173**, 851–856.
- Ilmas, E. R. & Savikhina, T. I. (1970). *J. Lumin.* **1/2**, 702–715.
- Johnson, C. D. (1990). *The Development and Use of Alumina Ceramic Fluorescent Screens*, CERN/PS/90–42(AR). European Laboratory for Particle Physics, Geneva, Switzerland.
- Leverenz, H. W. (1968). *An Introduction to Luminescence of Solids*, 1st ed. New York: Dover.
- Murakami, K. (1998). *Phosphor Handbook*, edited by S. Shionoya & W. M. Yen, pp. 433–443. Boca Raton: CRC Press.
- Osram Sylvania Inc. (1993). Yttrium Oxide: Europium Activated, Material Safety Data Sheet M0042. Osram Sylvania Inc., Towanda, USA.
- Popma, T. J. A., van der Weg, W. F. & Thimm, K. (1981). *J. Lumin.* **24/25**, 289–292.
- Tomiki, T., Fukudome, F., Kaminao, M., Fujisawa, M., Tanahara, Y. & Futemma, T. (1989). *J. Phys. Soc. Jpn.* **58**, 1801–1810.
- Zurro, B., Burgos, C., Ibarra, A. & McCarthy, K. J. (1997). *Fusion Eng. Des.* **34/35**, 353–357.
- Zurro, B., Burgos, C., McCarthy, K. J. & Rodriguez Barquero, L. (1997). *Rev. Sci. Instrum.* **68**, 680–682.